Developmental Cell, Volume *25*

Supplemental Information

Fuz Mutant Mice Reveal Shared Mechanisms between Ciliopathies and FGF-Related Syndromes

Jacqueline M. Tabler, William B. Barrell, Heather L. Szabo-Rogers, Christopher Healy, Yvonne Yeung, Elisa Gomez Perdiguero, Christian Schulz, Basil Z. Yannakoudakis, Aida Mesbahi, Bogdan Wlodarczyk, Frederic Geissmann, Richard H. Finnell, John B. Wallingford, and Karen J. Liu

Index of Supplemental Items:

Figure S1, related to Figure 1: This figure provides supporting data for Figure 1, including expression of *Patched1* in the palate and development of the palatine bones in mutants. To fully appreciate the anterior to posterior extent of the high arching palate, representative coronal sections through the palatin bone are shown. Also included are μCT reconstructions demonstrating the shape and size of the palatine bones.

Figure S2, related to Figure 3: This figure provides supporting data for Figure 3, showing similar levels of FGF8 expression in mutant and wildtype embryos prior to neural crest emigration. This figure also demonstrates a requirement for Fuz in *Fgf8* regulation in *Xenopus* embryos.

Figure S3, related to Figure 4: This figure shows supporting data for Figure 4, including an example of a nearly complete rescue of the *Fuz* mutant palate by *Fgf8* heterozygosity. Polydactyly is not rescued, suggesting that this phenotype is not dependent on FGF8.

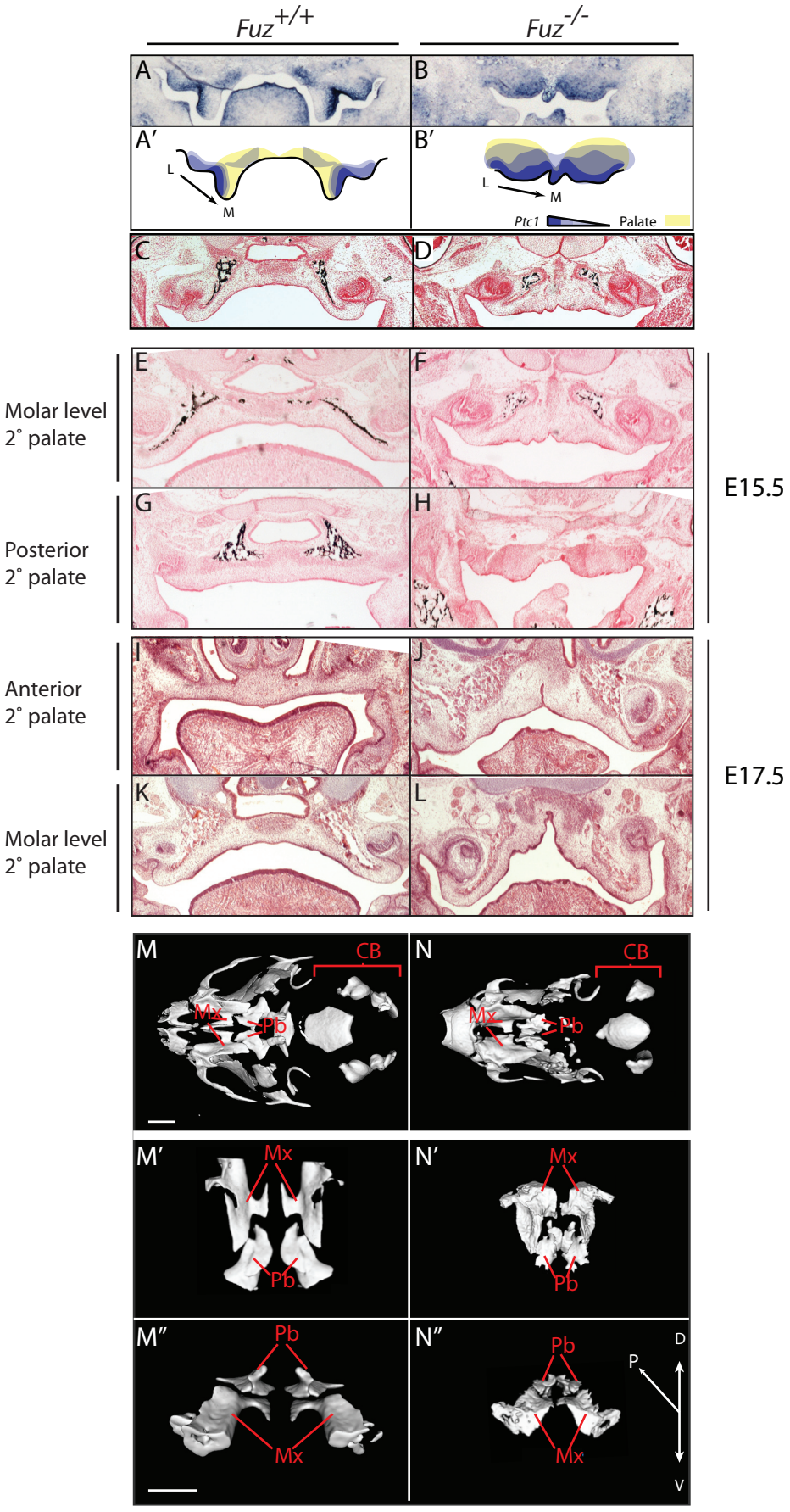

Tabler et al. Supplemental Figure 1

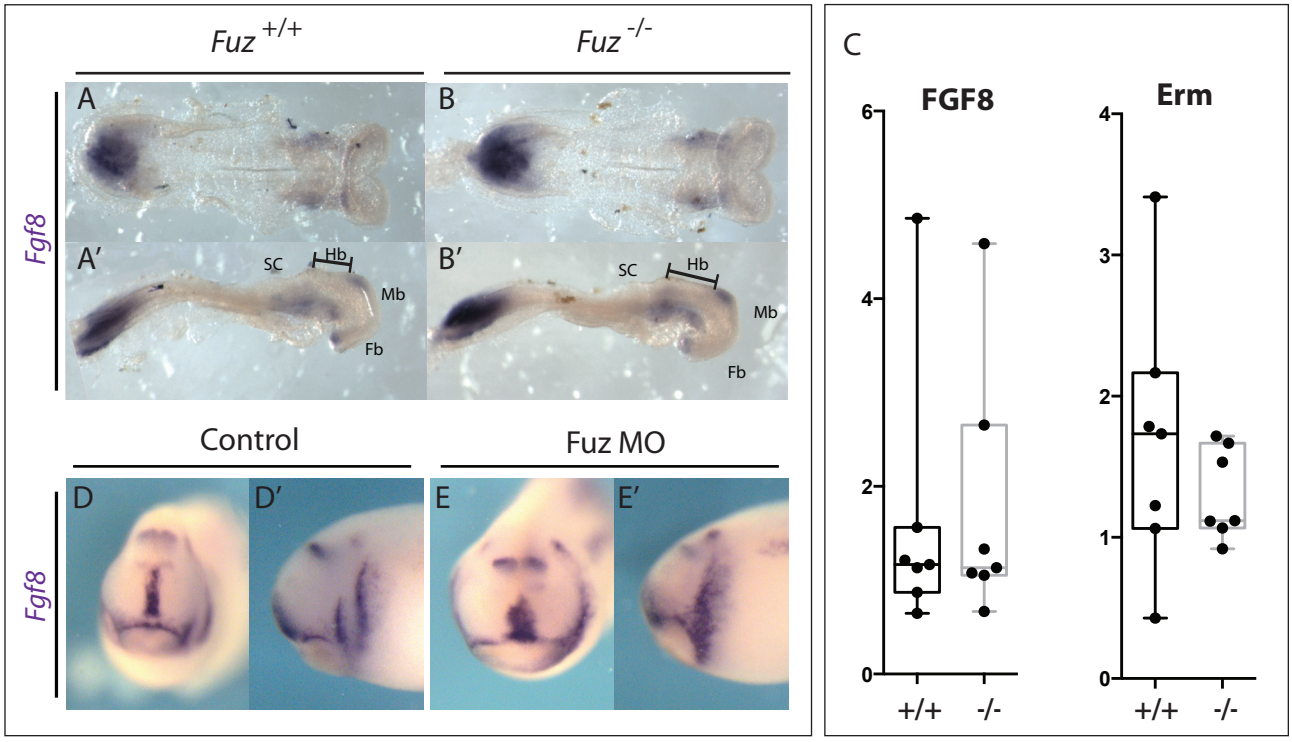

Tabler et al., Supplemental Figure 2

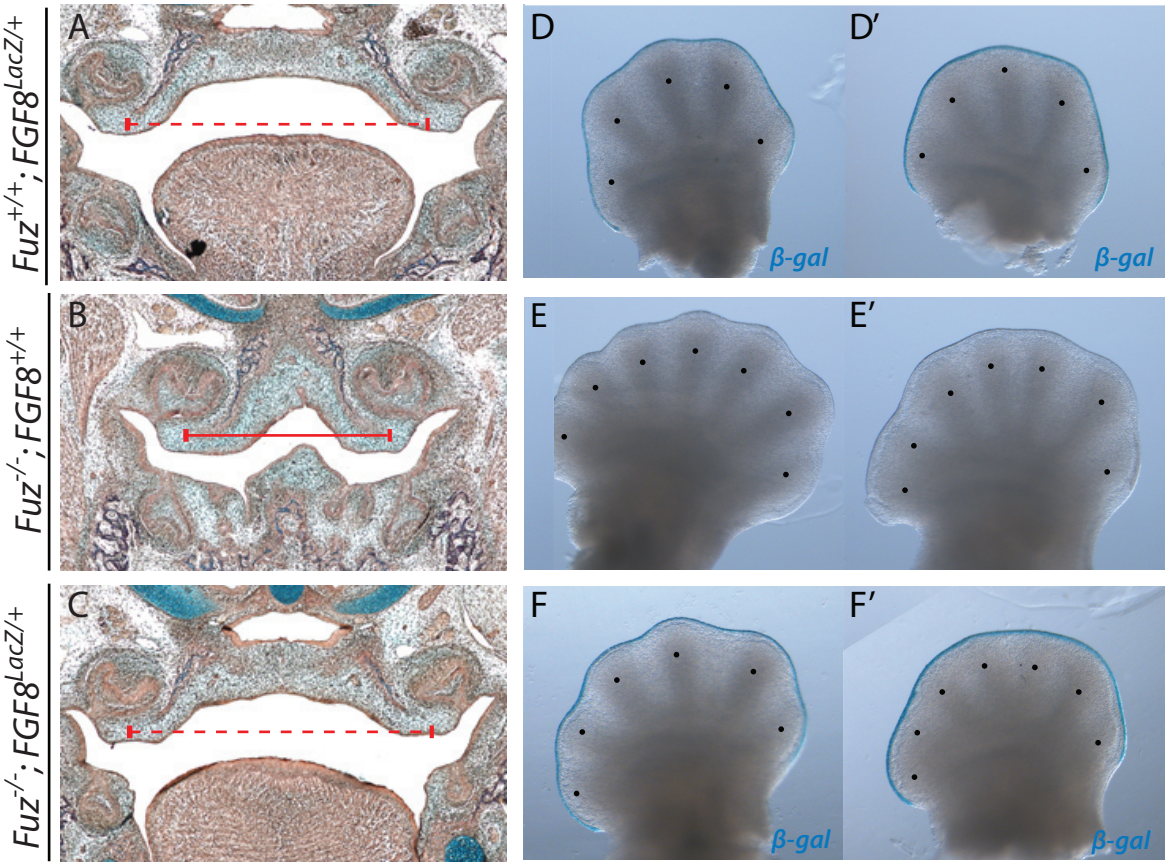

Tabler et al. Supplemental figure 3

SUPPLEMENTAL FIGURES:

Figure S1, related to Figure 1. Expression of Patched 1 and subsequent ossification of the palatine bone are maintained in *Fuz* mutants. A-B. mRNA *in situ* hybridization for *Patched1 (Ptc1),* E14.5. In controls, *Ptc1* is expressed in the lateral palatal mesenchyme. In mutants, *Ptc1* expression spans the midline. **A'-B'.** Schematic depiction of *Ptc1* expression (purple) in control and mutant palates suggesting a medial shift of the palatal shelves (yellow). L=lateral, M=medial. **C-D.** Von Kossa (black) stains ossified bone, E15.5. Bilateral ossification of the palatine bones is evident in both control and mutant sections. Mutant palatine bones are medially shifted. **Palatine bones are mediolaterally constrained throughout the anterior-posterior extent of the secondary palate in *Fuz* mutants. E-H.** Von Kossa staining of coronal sections showing the secondary palate at the level of the molars (E, F) and posterior to the molars (G-H) at E15.5. Palatine width and bone angle are decreased in mutant anterior palates compared to controls. No bone is observed in the most posterior extent of the secondary palate in mutants indicating a posterior shortening of the palatine bone compared to controls. **I-L**. H&E staining of coronal sections at the level of the anterior (I, J) and molar levels of the palate (K, L) in mutants at E17.5. Palatine width and bone angle are decreased throughout the secondary palate in *Fuz* mutants compared to controls (Compare J, L to I and K, respectively). **Palatine and maxillary bones are present in *Fuz* mutants.** μCT reconstruction of E17.5 WT and mutant cranial skeleton. **M-N.** Ventral views of the maxillary cranial skeleton and cranial base. Palatine and maxillary bones (Pb and Mx, respectively) are bilateral and extend antero-posteriorly. Bilateral palatine and maxillary bones can be observed in *Fuz* mutants, however they are constrained medio-laterally. Bones comprising the posterior cranial base (CB) are absent or reduced in size in mutants compared to controls (N compared to M). **M'-N'.** Reconstructions of only the maxillary and palatine bones reveal that, in mutants, both bones are correctly positioned, relative to eachother (N' compared to M'). In addition, the maxillary bone forms a bilateral, winged bone pair, similar in shape to controls, although Mx and Pb are reduced in size, are ossified across the midline and are constrained mediolaterally. **M''-N''.** Anterior views of Mx and Pb. D, V and P indicate dorsal, ventral and posterior, respectively. Mx and Pb are similar in shape in *Fuz* mutants compared to controls. Relative dorsal-ventral length of Pb is increased in mutants. These

reconstructions reveal that anterior-posterior patterning is retained in the *Fuz*$^{-/-}$ palates, suggesting that appropriate ossification cues are present. Scale bar indicates 100μM.

Figure S2, related to Figure 3. *Fuz* mutants exhibit normal *Fgf* expression levels prior to E9.0. *Fgf8 in situ* hybridization in E8.25 embryos. **A-B.** Dorsal views show *Fgf8* expression domains in the tailbud, prospective branchial arch epithelium, hindbrain (Hb) and rostral forebrain. *Fgf8* expression appears unchanged in mutant embryos at E8.25 **A'-B'.** Lateral views show hindbrain length in *Fuz* mutants compared to controls (black line, B' compared to A'). Relative mRNA levels are normalised against β-actin. *Fgf8* and *Erm* are unchanged at E9.0 in mutants (C, grey) compared to controls (C, black). Whiskers represent the maximum and minimum data values, while the 75, median and 25 percentile are represented in the box. ***FGF8* mRNA *in situ* hybridization of *Xenopus* embryos. D-E.** Lateral views of st. 24 embryos, controls or injected with antisense morpholino oligonucleotides (MO) targeting Fuz. In controls, *Fgf8* is expressed in branchial arch epithelia in discrete stripes in addition to anterior forebrain. Fuz MO injection expanded *Fgf8* expression domains. The two stripes of *Fgf8* expression are now merged (B, arrowhead). **D'-E'.** Frontal view. Anterior expression was expanded mediolaterally in Fuz morphants. Fuz morphant faces appear to be wider.

Figure S3, related to Figure 4. *Fgf8* reduction rescues maxillary hyperplasia and palatal width in compound mutants. A-C Trichrome staining of coronal sections of E16.5 embryos. Palatal width and bone angle are decreased in mutant embryos (B) compared to controls (A). Palatal width in *Fuz*$^{-/-}$*; Fgf8*$^{LacZ/+}$ (C) appears normal compared to controls (A). Angle of palatine bone is rescued when compared to controls (C compared to A and B). C represents best palatal rescue in compound mutants. ***Fgf8* reduction does not rescue polydactyly, in compound mutants, related to Figure 6.** Heterozygous *lacZ* knock in to the *Fgf8* locus drives expression of *β*-gal in BA1 epithelium (blue). **D-F.** Forelimbs**. D'-F'.** Hindlimbs. Limbs of *Fgf8*$^{LacZ/+}$ embryos are normal, black dots indicate five condensations. *Fuz*$^{-/-}$ mice are polydactylous (E-E') as are compound *Fuz*$^{-/-}$*; Fgf8*$^{LacZ/+}$ embryos (F-F'). β-gal expression reveals *Fgf8* expression in the apical ectodermal ridge.